

Studies on the Structure and Properties of Nylon 46 Fiber.

I. Dimensional Stability

KAZUSHIGE KUDO, MASATSUGU MOCHIZUKI, SHUNICHI KIRIYAMA, MASAHARU WATANABE, and MATSUO HIRAMI*

Research and Development Center, Unitika Ltd., 23 Kozakura, Uji, Kyoto 611, Japan

SYNOPSIS

Thermal shrinkage, viscoelastic properties, wide- and small-angle X-ray diffractions, and molecular orientation by fluorescence method were measured for fiber samples of nylon 46 [poly(tetramethylene adipamide)] as compared with nylon 66 [poly(hexamethylene adipamide)]. The structural study of nylon 46 fiber indicated that molecular chains are well-oriented along the fiber axis in the interlamellar region whose thickness is relatively thin. It was also shown that the onset of thermal movement of nylon 46 molecules is shifted to the higher temperature than nylon 66. These characteristics will be attributed to the cause of good dimensional stability, a significant feature of nylon 46 fiber, attractive for its application to industrial usages. © 1994 John Wiley & Sons, Inc.

INTRODUCTION

Nylon 46 [poly(tetramethylene adipamide)] was studied early by Carothers¹ as well as nylon 66 [poly(hexamethylene adipamide)].² Since then, however, nylon 46 has not been well developed in contrast to the success of nylon 66 as a commercial product.³ The difficulty of obtaining a high-molecular-weight polymer was a main obstacle for the industrial development of nylon 46. This difficulty has been overcome markedly by a recent progress of polymerization technology.⁴ In addition, an advance in fiber-making technology enables us to develop nylon 46 fiber to be commercialized as a new-generation nylon.⁵

Nylon 46 fiber has significant features such as a high melting temperature, good thermal stability, and good dimensional stability. We have studied the structure and properties of nylon 46 fiber in order to clarify, first, how these features are realized in relation to its structural characteristics and, second, how they are utilized as attractive performances for practical applications. In previous studies,⁶⁻⁸ we described the mechanical properties of nylon 46 fiber

with the emphasis of their good trends at high temperatures.

In this study, we report measurements of thermal shrinkage, viscoelastic properties, wide-angle X-ray diffraction (WAXD), small-angle X-ray diffraction (SAXD), and molecular orientation by fluorescence polarization method for nylon 46 fiber compared with nylon 66 fiber as a control.

Experimental results were examined for the elucidation of features of nylon 46 fiber, especially good dimensional stability. A brief discussion is given on the validity of the comparative study on fiber samples of nylon 46 and nylon 66.

EXPERIMENTAL

Characterization of Polymers

Amino end groups were determined by titration of nylon 46 solution in *m*-cresol with toluene sulfonic acid. Carboxyl end groups were determined by titration of nylon 46 solution in ethylene glycol/benzyl alcohol mixture with benzyl alcohol at an elevated temperature.⁹ In addition, pyrrolidine end groups were measured in a similar way reported by Roerdink and Warnier.¹⁰ Number-average molecular weight \bar{M}_n was obtained from data of amino, carboxyl, and pyrrolidine end groups.

* To whom all correspondence should be addressed.

Relative viscosities η_{rel} were measured with an Ubbelohde capillary viscometer at a concentration of 1 g/100 mL in 96% sulfuric acid at 25°C. Weight-average molecular weight \bar{M}_w was obtained from η_{rel} by applying the relationship of Roerdink and Warner,¹⁰ namely,

$$\bar{M}_w = 16.24 \times 10^3 (\eta_{\text{rel}} - 1)^{0.926} \quad (1)$$

Number-average molecular weight of nylon 66 was obtained from viscosity data with the use of the relationship of Ogata.¹¹ Weight-average molecular weight \bar{M}_w was estimated by doubling the value of \bar{M}_n based on the assumption of $\bar{M}_w/\bar{M}_n \cong 2$.

Measurements of differential scanning calorimetry (DSC) were made with the use of a Perkin-Elmer DSC-2/TAD.¹² The value of melting temperature T_m was read from the peak position of endothermic pattern on heating process in DSC. The program was set so as to heat at the rate of 10°C/min from room temperature to T' , to stay at T' for 5 h and then to heat at 2.5°C/min from T' , where 280°C was assigned to T' for nylon 46 and 240°C for nylon 66. The value of crystallization temperature T_c was read from the peak position of exothermic pattern on cooling process, where three different rates of cooling were employed, namely, 40, 80, and 160°C/min.

Preparation of Fiber Samples

Fiber samples of nylon 46 (840 den./140 fil.) were obtained by using a spin-draw equipment in our laboratory. Polymer resins of a high molecular weight of nylon 46 were supplied by DSM in the Netherlands. The polymer resins were dried, melted in a screw extruder, melt-spun from a spinneret, submitted continuously to the subsequent drawing stage with heating, and wound up by a high-speed winder.

Fiber samples of nylon 66 (840 den./140 fil.) were prepared also in our laboratory with the use of the same equipment of fiber making. For the preparation of both fiber samples of nylon 46 and nylon 66, various parameters that control the spinning and drawing stages were assigned almost the same values.

Characterization of Fiber Samples

Stress-strain curves were measured by Instron-model 1122.

Measurements of thermal shrinkage were made for looped samples prepared by tying together both ends of fiber yarns based on measurements of loop

length applying the load of (1/20) grams of yarn denier before and after heat treatment of the samples. Heat treatments at different temperatures were made by keeping the samples freely in a dry-oven for 15 min.

Dynamic mechanical properties were measured with the use of Rheovibron DDV-II (Toyo Baldwin) at the heating rate of 10°C/min under the constant tension of 5×10^{-3} kg/yarn.

The heat of fusion ΔH was obtained from the area under the peak of DSC diagram, where DSC measurements were made with the heating rate of 10°C/min for the samples prepared by cutting fiber yarns into short pieces.

Birefringence measurements were made by the retardation method with the use of a polarization microscope.

Measurements of WAXD and SAXD were made by Rigaku Denki-model RAD-rB with Ni-filtered $\text{Cu}\alpha$ radiation of 50 kV and 200 mA. SAXD data were obtained by using a small-angle goniometer with line collimators at the distance of 300 mm, where dimensions of the first and second slits were 12×0.5 and 12×0.3 mm.

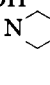
Measurements of the angular distribution of polarized components of fluorescence intensity emitted from fiber samples were made with the use of an apparatus of POM (Japan Spectroscopy Co.). The filter consists of color glass filter passing 365 nm mercury light and sharp cut-off filter passing fluorescence light only. Fiber samples were immersed in water containing fluorescent molecules, Whitex RP (Sumitomo Chem. Co.) at 0.2% on weight fiber, then dried for 24 h at 20°C and 65% relative humidity (RH).

RESULTS AND DISCUSSION

Table I and Table II show polymer characterization data for nylon 46 and nylon 66. We employ ΔT as a parameter, defined as the difference between T_m and T_c , which represents the rate of crystallization. Values of ΔT for nylon 46 and nylon 66, listed in Table II, are plotted against the rate of cooling in Figure 1. The smaller values of ΔT for nylon 46 indicate the higher rate of crystallization of this material.

For fiber samples of nylon 46 and nylon 66 obtained, stress-strain curves at various temperatures are shown in Figure 2. As the measure of the vertical axis in Figure 2, the standard unit of CN/d tex is added to the practical unit of g/d. Note that the values of tenacity (stress at break) for both fiber

Table I Polymer Characterization Data¹

	Nylon 46	Nylon 66	
End-group analysis (ends/10 ⁶ g)	—NH ₂	10.6	—
	—COOH	47.9	—
	—C—N 	16.1	—
Relative viscosity η_{rel} (100 ml/g)	3.63	—	
Molecular weight			
Number average \bar{M}_n	26,800	23,800	
Weight average \bar{M}_w	39,700	47,600	

samples observed at room temperature were adjusted to be the same, that is, 8.0 g/d. Consequently, the nylon 66 fiber gives the longer strain at a given stress, while the nylon 46 the higher stress at a given strain. This tendency at room temperature is enhanced at higher temperatures.

In Figure 3, data of thermal shrinkage for fiber samples of nylon 46 and nylon 66 are plotted against temperature T (°C) in the region of $120 \leq T \leq 200$. The trend of the lower thermal shrinkage for nylon 46 compared with nylon 66 is markedly enhanced with the increase of T . A significant feature of nylon 46 fiber, that is, the remarkably low thermal shrinkage, which means good dimensional stability, is very attractive for various usages of industrial applications.

For dynamic viscoelasticity of nylon 46 and nylon 66 fibers, dynamic modulus E' and loss modulus E'' plotted against T are shown in Figure 4. From the low to intermediate regions of T , E' of nylon 46 fiber is the same as that of nylon 66, then the latter decreases faster with the increase of T . As can be seen from the diagram of E'' vs. T , the main dispersion of nylon 46 is located at the higher temperature region by ca. 20°C as compared with nylon 66. This fact means that the onset of thermal movement of

nylon 46 molecules is shifted to the higher temperature than nylon 66.

In Table III, we present data of structural characteristics for fiber samples of nylon 46 and nylon 66. Figure 5 shows SAXD diagram for these samples, where the intensity of the diagram was calibrated by subtracting the contribution from background scattering. As for WAXD data, the apparent crystal size (ACS) was estimated from the half-height width of diffraction profiles.¹³ The values of ACS of nylon 46 crystals were estimated for (100), (110) + (010), and (014) planes¹⁴ and those of nylon 66 crystals were also estimated for (100), (110) + (010), and (015) planes.¹⁵ The degree of orientation (DO) was estimated from the half-height width of intensity profile along the Debye diffraction ring of (100) plane.¹⁶ The long period (LP), that is, the spacing of SAXD, was estimated from the Bragg spacing read at the position of maximum intensity in the profile of SAXD. The interlamellar thickness (IT) was estimated by the relationship

$$(IT) = (LP) - (ACS-3) \quad (2)$$

where (ACS-3) means the apparent crystal size along the fiber axis obtained from WAXD data,

Table II Polymer Characterization Data²

		Nylon 46	Nylon 66
Melting temperature (°C)	T_m	307	267
Crystallization temperature (°C)	T_c^{*1}	262	215
	T_c^{*2}	252	203
	T_c^{*3}	233	177
Rate of crystallization: $\Delta T = T_m - T_c$	ΔT^{*1}	45	52
	ΔT^{*2}	55	64
	ΔT^{*3}	74	90

*1, *2, and *3 attached to T_c and ΔT indicate three different rates of cooling, namely 40, 80, and 160°C/min.

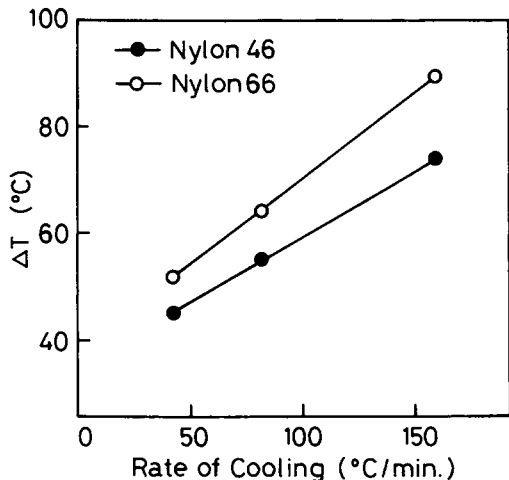


Figure 1 Plot of $\Delta T = T_m - T_c$ against the rate of cooling for nylon 46 and nylon 66.

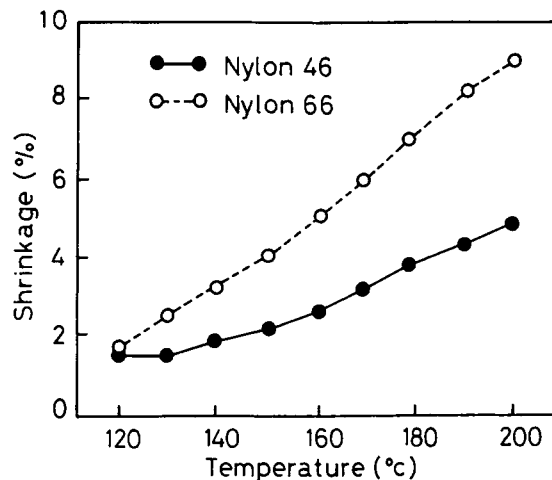


Figure 3 Thermal shrinkage for fiber samples of nylon 46 and nylon 66 plotted against temperature.

namely (ACS) of (014) plane for nylon 46 and (015) plane for nylon 66, respectively.

From the heat of fusion ΔH , the degree of crystallinity (DC) was estimated by the relationship,

$$DC(\%) = (\Delta H / \Delta H_c) \times 100 \quad (3)$$

where ΔH_c is the heat of fusion for the purely crystalline part of a semicrystalline polymer. The value

of ΔH_c for nylon 46 and nylon 66 was assigned to 210 J/g and 196 J/g, cited from the literature of Gaymans et al.¹⁴ and Wilheit et al.,¹⁷ respectively.

From these data, the following results were obtained:

- (i) The crystal size of nylon 46 along the fiber axis is a little shorter than that of nylon 66.

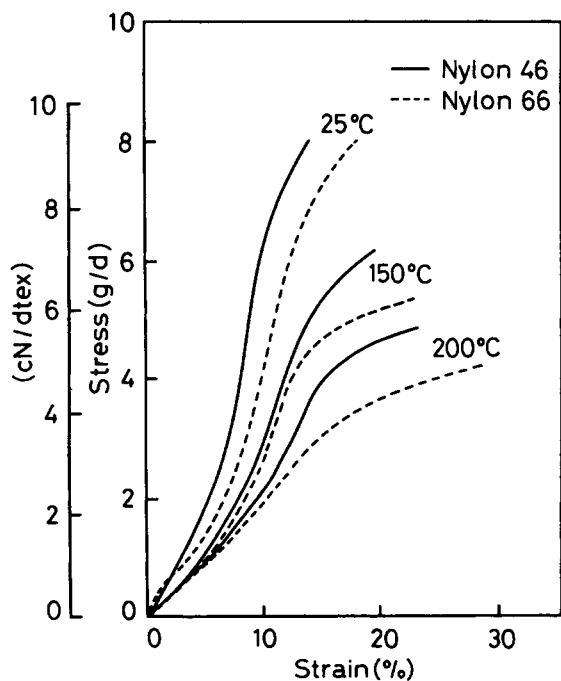


Figure 2 Stress-strain curves at various temperatures for fiber samples of nylon 46 and nylon 66.

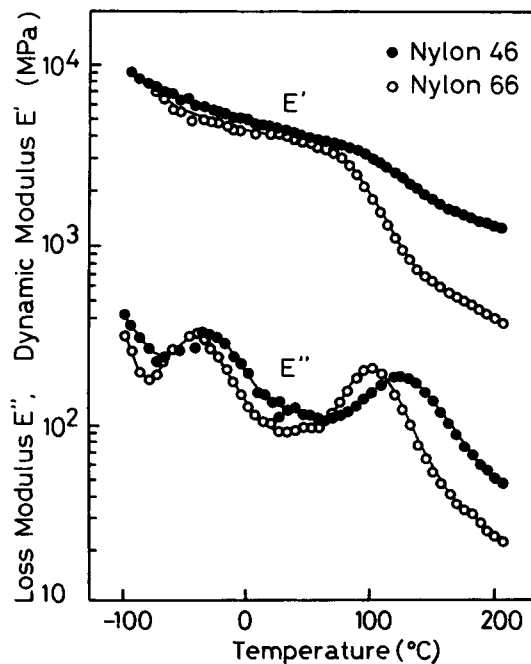


Figure 4 Dynamic modulus E' and loss modulus E'' for fiber samples of nylon 46 and nylon 66 plotted against temperature.

Table III Structural Data for Fiber Samples

	Nylon 46	Nylon 66
WAXD		
ACS-1 ^a	33	41
ACS-2 ^b	25	28
ACS-3 ^c	63	67
DO (%) ^d	93.4	94.0
SAXD		
LP (Å) ^e	84	98
IT (Å) ^f	21	31
Birefringence ($\times 10^3$)	63	60
ΔH (J/g) ^g	109	79
DC (%) ^h	52	40

^a ACS (apparent crystal size) for (100) plane.

^b ACS for (110) + (010).

^c ACS for (014) of nylon 46 and for (015) of nylon 66.

^d Degree of orientation estimated from the profile of (100) plane.

^e Long period, i.e., the spacing of SAXD.

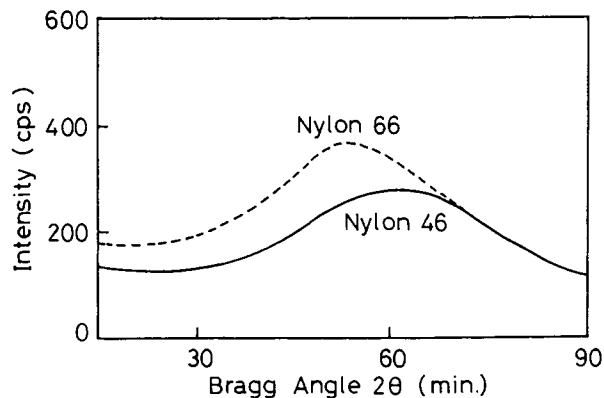
^f Interlamellar thickness. See Eq. (2).

^g Heat of fusion.

^h Degree of crystallinity. See Eq. (3).

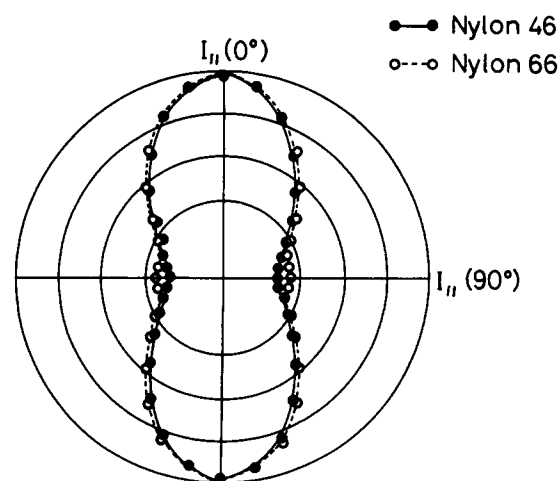
- (ii) The long period, that is, the SAXD spacing of nylon 46 is shorter than that of nylon 66.
- (iii) The thickness of interlamellar layer of nylon 46 is remarkably thin, namely about two thirds compared with nylon 66.
- (iv) The intensity of SAXD, which roughly corresponds to the difference in electron density between crystalline and noncrystalline regions, is smaller for nylon 46 than for nylon 66.
- (v) The degree of crystallinity estimated from DSC data of nylon 46 is higher than that of nylon 66.
- (vi) The combination of birefringence and the degree of orientation estimated from WAXD data suggests that the orientation in the interlamellar layer, that is, the amorphous (noncrystalline) region between lamellar crystals is higher for nylon 46 than for nylon 66.

In order to provide further information that will be useful for the examination of the morphology described in the above (vi), we have investigated the orientation of molecular chains in the interlamellar layer by means of the fluorescence polarization method. According to the procedure developed by Nishijima et al.,¹⁸ we consider $I_\theta(\omega)$, the angular distribution of the polarized component of fluorescence intensity, where θ is the angle between the

**Figure 5** SAXD diagram for fiber samples of nylon 46 and nylon 66.

direction of plane-polarized incident beam, namely the direction of the exciting vector \mathbf{OP}_1 , and the direction in which the intensity of the polarized component of fluorescence is observed through an analyzer with its electric vector \mathbf{OP}_2 , and ω is the angle between the direction of vector \mathbf{OP}_1 and the axis of orientation. From $I_\theta(\omega)$, we can obtain the parallel component $I_{\parallel}(\omega)$ for $\theta = 0$ and the perpendicular component $I_{\perp}(\omega)$ for $\theta = \pi/2$. In the present study, however, we are concerned with only the parallel component $I_{\parallel}(\omega)$. Figure 6 shows the angular distribution of $I_{\parallel}(\omega)$ for fiber samples of nylon 46 and nylon 66. We introduce the parameter f defined as

$$f = I_{\parallel}(\omega = 0) / I_{\parallel}(\omega = \pi/2) \quad (4)$$

**Figure 6** Angular distribution of the parallel component of fluorescence polarization $I_{\parallel}(\omega)$ for fiber samples of nylon 46 and nylon 66. $I_{\parallel}(\theta)$ and $I_{\parallel}(\pi/2)$ are indicated in the figure.

which can be used as an index for the orientation of molecular chains in noncrystalline regions. As can be seen from Figure 6, the parameter f for nylon 46 fiber is appreciably higher than for nylon 66, and this finding strongly supports the results deduced from WAXD, SAXD, and birefringence data.

Finally, we wish to make a comment on whether the comparative study on fiber samples of nylon 46 and nylon 66 presented in this article will be valid with generality. The structure and properties of a fiber sample depend markedly on a number of conditions during the course of the fiber-making process. Therefore, several kinds of fiber samples for the comparative study, namely nylon 46 and nylon 66 in this case, have to be prepared according to some references of standard.

The references in the present work are as follows:

- (i) As starting materials of both fiber samples, we chose polymer grades of nylon 46 and nylon 66, whose molecular weights are approximately the same, that is, $\bar{M}_n \cong 25,000$.
- (ii) We employed the policy that various factors for both fiber samples, which cause the structural development on the process of fiber formation such as the rate of deformation and heating temperatures, should be on the same level.
- (iii) As a fundamental performance figure of fiber products, the tenacity values of both fiber samples were adjusted so as to be the same, that is, 8.0 g/d.

Among these three items, (i) and (ii) are scientifically important, while (iii) is a useful reference for studying applications. Based on the above considerations, we believe that our discussion on the structure and properties of nylon 46 fiber in comparison to nylon 66 fiber will have a reasonable validity.

CONCLUDING REMARKS

Summarizing the results obtained, the features of the structure formation in nylon 46 fiber will be described as follows. In as-spun fiber of nylon 46, a number of crystal nuclei are formed due to the high rate of crystallization. In general, the remarkable reorganization of structural framework occurs during the course of the drawing process due to the orientation effect of molecular chains along the fiber axis. Nevertheless we may presume that some structural characteristics inherent in as-spun fiber,

formed on the crystallization process from the melt, still remain even after drawing. Then a number of crystal nuclei formed in as-spun fiber will result in the morphology consisting of a number of lamellar crystals in the drawn fiber of nylon 46. This corresponds to the small value of long period obtained from SAXD data.

The crystal size estimated from WAXD data does not differ so much from that of nylon 66. This is probably caused by the restriction of crystal growth beyond the critical nucleus, despite the high rate of crystallization for nylon 46. Thus it is naturally understood that the degree of crystallinity for nylon 46 is higher than for nylon 66, deduced from the combination of SAXD and WAXD data.

As for the interlamellar layer, the principal features are that (i) the thickness of the layer is thin, (ii) molecular chains in the layer are well-oriented, and (iii) the compactness of the layer is relatively high. The feature of (ii) was suggested by the combination of birefringence and WAXD data, and later confirmed by the fluorescence polarization method. The feature of (iii) is reflected on the low intensity in SAXD profile.

Due to its high melting temperature, nylon 46 should possess a high glass transition temperature, regarded as a significant feature of this material. Indeed, as compared with nylon 66, the onset of thermal movement of nylon 46 molecules is shifted to the higher temperature. This was proved by rheological data of dynamic viscoelasticity.

The structural, morphological, and rheological features of nylon 46 fiber presented so far leads to its excellent performance of good dimensional stability, attractive for the application to industrial usages.^{7,8} The potential of nylon 46 fiber as a new-generation nylon was recently discussed elsewhere.¹⁹

The crystal structure of nylon 46, closely related to its high melting temperature, will be examined in a subsequent work.

REFERENCES

1. W. H. Carothers, E. I. du Pont de Nemours and Co., U.S. Pat. 2,130,948 (Sept. 20, 1938).
2. H. F. Mark and G. S. Whitby Eds., *Collected Papers of Wallace Hume Carothers on High Polymeric Substances*, Interscience Publishers, Inc., New York, 1940, Part One, p. 179.
3. H. Hopff, in *Man-Made Fibers, Science and Technology*, H. F. Mark, S. M. Atlas, and E. Cernia, Eds., Vol. 12, Wiley, New York, 1967, Chap. 7.
4. The progress of polymerization was developed by DSM (the Netherlands). The original patents are U.S. Pat. 4,460,762 and 4,408,036, (Mar. 26, 1980). R. J.

- Gaymans et al., Stamicarbon (a subsidiary company of DSM).
- Unitika and DSM have jointly developed nylon 46 fiber. The polymer production of nylon 46 was commercialized by DSM in 1990 and the fiber production of nylon 46 by Unitika was started in 1992.
 - M. Watanabe and M. Hiram, Presented at the Annual Symposium of Rubber and Elastomer Division, American Chemical Society, Atlanta, GA, Oct. 9, 1986.
 - K. Kudo and M. Mochizuki, Presented at 3rd International TECHTEXTIL-Symposium, Frankfurt, Germany, May 14, 1991.
 - M. Mochizuki and K. Kudo, *Sen-i Gakkaishi*, **47**, 336 (1991).
 - R. J. Gaymans, T. E. C. van Utteren, J. W. A. van den Berg, and J. Schuyer, *J. Polym. Sci., Polym. Chem. Ed.*, **15**, 537 (1977).
 - E. Roerdink and J. M. M. Warnier, *Polymer*, **26**, 1582 (1985).
 - N. Ogata, *Makromol. Chem.*, **42**, 58 (1960).
 - B. Ke, in *Newer Methods of Polymer Characterization*, B. Ke, Ed., Interscience, New York, 1964, Chap. 9.
 - L. E. Alexander, *X-Ray Diffraction Methods in Polymer Science*, Wiley, New York, 1969, p. 335.
 - R. J. Gaymans, D. K. Doeksen, and S. Harkema, in *Integration of Fundamental Polymer Science and Technology*, L. A. Kleintjens and P. J. Lemstra, Eds., Elsevier Applied Science Publishers, London and New York, 1985, p. 573.
 - C. W. Bunn and E. V. Garner, *Proc. Roy. Soc.*, **A189**, 39 (1947).
 - L. E. Alexander, *X-Ray Diffraction Methods in Polymer Science*, Wiley, New York, 1969, p. 262.
 - R. C. Wilhoit and M. Dole, *J. Phys. Chem.*, **57**, 14 (1953).
 - Y. Nishijima, *J. Polymer Sci., Part C*, **31**, 353 (1970); Y. Nishijima, Y. Onogi, and T. Asai, *J. Polymer Sci., Part C*, **15**, 237 (1966); G. Oster and Y. Nishijima, in *Newer Methods of Polymer Characterization*. B. Ke, Ed., Interscience, New York, 1964, Chap. 5.
 - Candidates for the industrial application of nylon 46 fiber are sewing threads, in-rubber reinforcement (tire, belt, and hose), covering cloth, filters, felt, and dry canvas for paper making machine.

Received April 26, 1993

Accepted October 19, 1993